

No. 59

STUDY ON ENVIRONMENTAL IMPACT OF MINING ACTIVITIES AND COUNTERMEASURES IN THE UNITED MEXICAN STATES

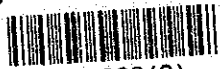
THE STUDY ON ENVIRONMENTAL IMPACT OF MINING ACTIVITIES AND COUNTERMEASURES IN THE UNITED MEXICAN STATES

FINAL REPORT

MARCH 1971

615
618
MTR

JICA LIBRARY



1098326 (0)

23828

THE STUDY
ON
ENVIRONMENTAL IMPACT
OF
MINING ACTIVITIES
AND
COUNTERMEASURES
IN
THE UNITED MEXICAN STATES
FINAL REPORT

MARCH, 1992

JAPAN INTERNATIONAL COOPERATION AGENCY

国際協力事業団

23828

PREFACE

In response to a request from the Government of United Mexican States, the Japanese Government decided to conduct the study on Environmental Impact of Mining Activities and Countermeasures and entrusted the study to the Japan International Cooperation Agency (JICA).

JICA sent a survey team to Mexico headed by Mr. Shigeru Hashimoto of Dowa Mining Co., Ltd. over three periods of January to March 1991, July to September 1991 and February 1992.

The team held discussions with the concerned officials of the Government of Mexico, and conducted field surveys. After the team returned to Japan, further studies were made and the present report was prepared.

I hope that this report will contribute to the promotion of the project and to the enhancement of friendly relations between our two countries.

I wish to express my sincerest appreciation to the officials concerned of the Government of Mexico for their close cooperation extended to the team.

March, 1992



Kensuke Yanagiya

President

Japan International Cooperation Agency

CONTENTS

1. Introduction	1
2. Outline of the Field Investigation	2
3. Survey Results and Countermeasures in the Area of El Bote	4
3-1 General Situation	4
3-2 Geology	5
3-3 Electrical Prospecting	10
3-4 Hydrology	11
3-5 Soil	23
3-6 Tailing Dam	25
3-7 Dust Problem	33
3-8 Summary of the Investigation	37
3-9 Measures against Mine Pollution	38
4. Survey Results and Countermeasures in the Area of Parral	48
4-1 General Situation	48
4-2 Geology	49
4-3 Electrical Prospecting	52
4-4 Hydrology	54
4-5 Soil	69
4-6 Tailing Dam	71
4-7 Dust Problem	77
4-8 Summary of the Investigation	79
4-9 Measures against Mine Pollution	81
5. Survey Results and Countermeasures in the Area of New El Coco	92
5-1 General Situation	92
5-2 Geology	92
5-3 Electrical Prospecting	99
5-4 Hydrology	101
5-5 Soil	115
5-6 Tailing Dam Model	117
5-7 Summary of the Investigation	120
5-8 Measures against Mine Pollution	121
6. Summary	129
Appendix A Numeriacal Simulation Technology for Subsurface Fluid Flow	

List of Figures

- Fig. 2-1 Location Map
- Fig. 2-2 Photographs of Survey Area
- Fig. 2-3 Progress in the Field Investigation (Dry Season)
- Fig. 2-4 Progress in the Field Investigation (Rainy Season)
- Fig.3-1-1 Hydrologic and Meteorologic Map
- Fig.3-2-1 Geological Plane Map
- Fig.3-2-2 Geological Cross Section
- Fig.3-2-3 Geologic Column
- Fig.3-2-4 Location Map of Boring Site
- Fig.3-2-5 Boring Log
- Fig.3-2-6 Location Map of Fissure Measuring Site
- Fig.3-2-7 Wulff's Net of Fissure Direction
- Fig.3-3-1 Location Map of Electrical Prospecting Station
- Fig.3-3-2 Resistivity Cross Section
- Fig.3-4-1 Location Map of Flow Rate Measurement and
Chemical Analysis of Water
- Fig.3-4-2 Surface Water Balance
- Fig.3-4-3 Analysis Map of Chemical Data of Water
- Fig.3-4-4 Micro Flow Analysis
- Fig.3-4-5 Analysis Map of Groundwater Reservoir (Plane)
- Fig.3-4-6 Analysis Map of Groundwater Reservoir (Cross Section)
- Fig.3-4-7 Location Map of Permeability Test Sample
- Fig.3-4-8 Groundwater Simulation Area
- Fig.3-4-9 Rock Classification Map
- Fig.3-4-10 Groundwater Saturation Map
- Fig.3-4-11 Groundwater Velocity Map
- Fig.3-5-1 Analysis Map of Chemical Data of Soil
- Fig.3-6-1 The Flow of Rainwater
- Fig.3-6-2 Boring and Soil Test Sample Point
- Fig.3-6-3 Grain Size Accumlation Curve
- Fig.3-6-4 El Bote Tailing Dam Geological Cross Section
- Fig.3-6-5 The Method for Presumption of Border Line
- Fig.3-6-6 The Model of Tailing Dam Stability Analysis

- Fig.3-6-7 A Result of Tailing Dam Stability Analysis (1)
- Fig.3-6-8 A Result of Tailing Dam Stability Analysis (2)
- Fig.3-6-9 A Result of Tailing Dam Stability Analysis (3)
- Fig.3-6-10 A Result of Tailing Dam Stability Analysis (4)
- Fig.3-6-11 The Scope for Danger of Liquefaction
- Fig.3-7-1 Location Map of Meteorological Station
- Fig.3-7-2 Location Map of Dust Jar Sampling
- Fig.3-7-3 Location Map of Low Volume Sampler
- Fig.3-7-4 Location Map of Digital Dust Monitors
- Fig.3-7-5 Analysis Map of Digital Dust Monitors
- Fig.3-9-1 The Model of Counter Load
- Fig.3-9-2 The Model of Tailing Dam Stability Analysis
- Fig.3-9-3 A Result of Tailing Dam Stability Analysis (1)
- Fig.3-9-4 A Result of Tailing Dam Stability Analysis (2)
- Fig.3-9-5 A Result of Tailing Dam Stability Analysis (3)
- Fig.3-9-6 A Result of Tailing Dam Stability Analysis (4)
- Fig.3-9-7 Drainage Plan
- Fig.3-9-8 Probability Precipitation
- Fig.3-9-9 Typical Cross Section of Drainage
- Fig.4-1-1 Hydrologic and Meteorologic Map
- Fig.4-2-1 Geological Plane Map
- Fig.4-2-2 Geological Cross Section
- Fig.4-2-3 Geologic Column
- Fig.4-2-4 Location Map of Boring Site
- Fig.4-2-5 Boring Log
- Fig.4-2-6 Location Map of Fissure Measuring Site
- Fig.4-2-7 Wulff's Net of Fissure Direction
- Fig.4-3-1 Location Map of Eletrical Prospecting Station
- Fig.4-3-2 Resistivity Cross Section
- Fig.4-4-1 Location Map of Flow Rate Measurement and
Chemical Analysis of Water
- Fig.4-4-2 Surface Water Balance
- Fig.4-4-3 Analysis Map of Chemical Data of Water
- Fig.4-4-4 Micro Flow Analysis

- Fig.4-4-5 Analysis Map of Groundwater Reservoir (Plane)
- Fig.4-4-6 Analysis Map of Groundwater Reservoir (Cross Section)
- Fig.4-4-7 Location Map of Permeability Test Sample
- Fig.4-4-8 Groundwater Simulation Area
- Fig.4-4-9 Rock Classification Map
- Fig.4-4-10 Groundwater Saturation Map
- Fig.4-4-11 Groundwater Velocity Map
- Fig.4-5-1 Analysis Map of Chemical Data of soil
- Fig.4-6-1 Boring and Soil Test Sample Point
- Fig.4-6-2 Grain Size Accumulation Curve
- Fig.4-6-3 Parral Tailing Dam Geological Cross Section
- Fig.4-6-4 The Model of Tailing Dam Stability Analysis
- Fig.4-6-5 A Result of Tailing Dam Stability Analysis (1)
- Fig.4-6-6 A Result of Tailing Dam Stability Analysis (2)
- Fig.4-6-7 A Result of Tailing Dam Stability Analysis (3)
- Fig.4-6-8 A Result of Tailing Dam Stability Analysis (4)
- Fig.4-6-9 The Scope for Danger of Liquefaction
- Fig.4-7-1 Location Map of Meteorological Station
- Fig.4-7-2 Location Map of Dust Jar Sampling
- Fig.4-7-3 Location Map of Low Volume Sampler
- Fig.4-7-4 Location Map of Digital Dust Monitors
- Fig.4-9-1 The Model of Counter Load
- Fig.4-9-2 The Model of Tailing Dam Stability Analysis
- Fig.4-9-3 A Result of Tailing Dam Stability Analysis (1)
- Fig.4-9-4 A Result of Tailing Dam Stability Analysis (2)
- Fig.4-9-5 A Result of Tailing Dam Stability Analysis (3)
- Fig.4-9-6 A Result of Tailing Dam Stability Analysis (4)
- Fig.4-9-7 Drainage Plan
- Fig.4-9-8 Drainage Section
- Fig.4-9-9 Typical Cross Section of Drainage
- Fig.4-9-10 Probability Precipitation
- Fig.5-1-1 Hydrologic and Meteorologic Map
- Fig.5-1-2 Temperature-Humidity Variation Diagram
- Fig.5-2-1 Geological Plane Map

- Fig.5-2-2 Geological Cross Section
- Fig.5-2-3 Geologic Column
- Fig.5-2-4 Location Map of Boring Site
- Fig.5-2-5 Boring Log
- Fig.3-2-6 Location Map of Fissure Measuring Site
- Fig.5-2-7 Wulff's Net of Fissure Direction
- Fig.5-3-1 Location Map of Electrical Prospecting Station
- Fig.5-3-2 Resistivity Cross Section
- Fig.5-4-1 Location Map of Flow Rate Measurement and
Chemical Analysis of Water
- Fig.5-4-2 Surface Water Balance
- Fig.5-4-3 Analysis Map of Chemical Data of Water
- Fig.5-4-4 Micro Flow Analysis
- Fig.5-4-5 Analysis Map of Groundwater Reservoir (Plane)
- Fig.5-4-6 Analysis Map of Groundwater Reservoir (Cross Section)
- Fig.5-4-7 Rainfall and Groundwater Level Variation Diagram
- Fig.5-4-8 Location Map of Permeability Test Sample
- Fig.5-4-9 Groundwater Simulation Area
- Fig.5-4-10 Rock Classification Map
- Fig.5-4-11 Groundwater Saturation Map
- Fig.5-4-12 Groundwater Velocity Map
- Fig.5-4-13 Rock Classification Map (after Setting up a Tailing Dam)
- Fig.5-4-14 Groundwater Saturation Map (after Setting up a Tailing Dam)
- Fig.5-4-15 Groundwater Velocity Map (after Setting up a Tailing Dam)
- Fig.5-5-1 Analysis Map of Chemical Data of soil
- Fig.5-6-1 Boring and Soil Test Sample Point
- Fig.5-6-2 Grain Size Accumulation Curve
- Fig.5-6-3 Model of New El Coco Tailing Dam
- Fig.5-8-1 The Model of Tailing Dam Stability Analysis
- Fig.5-8-2 A Result of Tailing Dam Stability Analysis (1)
- Fig.5-8-3 A Result of Tailing Dam Stability Analysis (2)
- Fig.5-8-4 A Result of Tailing Dam Stability Analysis (3)
- Fig.5-8-5 A Result of Tailing Dam Stability Analysis (4)
- Fig.5-8-6 Drainage Flow

- Fig.5-8-7 New El Coco Tailing Dam Drainage Plan
 Fig.5-8-8 Probablility Precipitation
 Fig.5-8-9 Typical Cross Section of Drainage

List of Tables

- Table 2-1 Total Amount of Electric Exploration and Boring Works
 Table 3-4-1 Hydrologic Measurment of Surface Water
 Table 3-4-2 Background and Water Supply Ceiling of Chemical Components
 in Water
 Table 3-4-3 Chemical Analysis of Surface Water
 Table 3-4-4 Micro Flow Measurement Data
 Table 3-4-5 Characteristic of Aquifer
 Table 3-4-6 Chemical Analysis of Groundwater
 Table 3-4-7 Permeability Coefficient Data
 Table 3-4-8 Permeability and Porosity Model
 Table 3-5-1 Chemical Analysis of Soil
 Table 3-6-1 Soil Test Quantity
 Table 3-6-2 Soil Test Data
 Table 3-6-3 Natural Moisture Content and Wet Density
 Table 3-6-4 Consistency Data of Soil
 Table 3-6-5 A Result of Tailing Dam Stability Analysis
 Table 3-7-1 Wind System Data
 Table 3-7-2 Wind Speed Data
 Table 3-7-3 Wind Direction Data
 Table 3-7-4 Dust Jar Measurement Data
 Table 3-7-5 Chemical Analysis of Falling Dust
 Table 3-7-6 Condition of Low Volume Air Sampler
 Table 3-7-7 Low Volume Air Sampler Measuremnt Data
 Table 3-7-8 Digital Type Dust Monitor Data
 Table 3-7-9 Comparative Data of Digital Type Dust Monitors
 Table 3-9-1 A Result of Tailing Dam Stability Analysis
 Table 3-9-2 Day Probablility Precipitation
 Table 4-4-1 Hydrologic Measurment of Surface Water
 Table 4-4-2 Background and Water Supply Ceiling of Chemical Components

In Water

- Table 4-4-3 Chemical Analysis of Surface Water
- Table 4-4-4 Micro Flow Measurement Data
- Table 4-4-5 Characteristic of Aquifer
- Table 4-4-6 Chemical Analysis of Groundwater
- Table 4-4-7 Permeability Coefficient Data
- Table 4-4-8 Permeability and Porosity Model
- Table 4-5-1 Chemical Analysis of Soil
- Table 4-5-2 Chemical Analysis of Solution Extracted
from the Soil Samples
- Table 4-6-1 Soil Test Quantity
- Table 4-6-2 Soil Test Data
- Table 4-6-3 Natural Moisture Content and Wet Density
- Table 4-6-4 Consistency Data of Soil
- Table 4-6-5 A Result of Tailing Dam Stability Analysis
- Table 4-7-1 Wind Speed Data
- Table 4-7-2 Wind Direction Data
- Table 4-7-3 Dust Jar Measurement Data
- Table 4-7-4 Condition of Low Volume Air Sampler
- Table 4-7-5 Low Volume Air Sampler Measurement Data
- Table 4-7-6 Digital Type Dust Monitor Data
- Table 4-9-1 A Result of Tailing Dam Stability Analysis
- Table 4-9-2 Day Probability Precipitation
- Table 5-4-1 Hydrologic Measurement of Surface Water
- Table 5-4-2 Background and Water Supply Ceiling of Chemical Components

In Water

- Table 5-4-3 Chemical Analysis of Surface Water
- Table 5-4-4 Micro Flow Measurement Data
- Table 5-4-5 Characteristic of Aquifer
- Table 5-4-6 Chemical Analysis of Groundwater
- Table 5-4-7 Permeability Coefficient Data
- Table 5-4-8 Permeability and Porosity Model
- Table 5-5-1 Chemical Analysis of Soil
- Table 5-6-2 Soil Test Quantity

Table 5-6-2 Soil Test Data

Table 5-6-3 Natural Moisture Content and Wet Density

Table 5-8-1 A Result of Tailing Dam Stability Analysis

Table 5-8-2 Day Probability Precipitation

1. Introduction

1. I N T R O D U C T I O N

In July 1990, The Government of the United Mexican States requested the Government of Japan to conduct an extensive study on "Environmental Impact of Mining Activities and Countermeasures in the United Mexican States" as a part of national policy in its mining industry. Based on this request, an agreement was made in August, 1990, as the Scope of Works (S/W) between the Government of the United Mexican States and Japan International Cooperation Agency (JICA), the official agency for the Government of Japan, to realize this technical cooperation program.

The main objective of the Study is, as indicated in the above S/W and the instruction given by JICA in December, 1990, to formulate appropriate environmental protection measures at the mining sites through the following investigations of present environmental condition.

- (1) Investigation on environmental influence of tailing dams by collapse of embankment and outflow of waste materials.
- (2) Investigation on contamination of surface and ground water by mine effluent.
- (3) Investigation on scattering dust particles carried away by the wind from tailing dams.

Technology transfer to the Mexican counterparts assigned in this study is also included throughout the program.

This Final Report describes present environmental situation obtained from the field investigation performed over dry and rainy seasons and practical, appropriate countermeasures for improvement.

2. Outline of the Field Investigation

2. OUTLINE OF THE FIELD INVESTIGATION

Field investigation was planned in two stages, in dry and rainy season. The first part was carried out in dry season from Jan. 21st (Mon) to March 27th (Wed), 1991, for 66 days and the second was in rainy season from July 15th (Mon) to Sept. 18th (Wed) for another 66 days. The survey areas were the following three mining sites as designated in the S/W, shown in Fig.2-1 and Fig.2-2.

- (1) El Bote tailing dam, State of Zacatecas (hereafter referred to El Bote)
- (2) Parral tailing dam, State of Chihuahua (Parral)
- (3) El Coco new tailing dam (proposed) site, State of Sinaloa (New El Coco)

Principal objects of the survey were as follows.

- (a) Collection of data regarding topography, geology, meteorology, mineral processing plant and tailing dam
- (b) Geological reconnaissance in and around the survey areas
- (c) Study on geology and ground water movement through electric exploration
- (d) Study on geology and ground water movement through boring works
- (e) Measurement of flow rate and velocity of surface and ground water
- (f) Analysis of chemical components contained in the surface and ground water
- (g) Physical properties of soil constituting tailing dam
- (h) Physical properties of soil around New El Coco dam construction site
- (i) Analysis of chemical components like heavy metal ions, contained in the soil
- (j) Scattering of dust fall from the existing tailing dam

Based on these technical data obtained through the survey, following matters were analysed and investigated collectively.

1. Local hydrographic system including surface and ground water (a ~ f)
2. Influence of dam effluent and penetration on the adjacent area (a ~ f, h)
3. Evaluation for physical stability of the existing dams (g)
4. Constructive estimation for the proposed dam site (h)
5. Environmental influence of dust fall from the existing dams (j)

The above-mentioned investigation matters are almost common to the three areas, however, actual survey plans were finally decided after considering local situation in each area and adopting CFM's request as far as possible through successive discussions. Also some modification was made in each area due to limit of the working days.

Electric exploration and boring works were actually performed by local contractors after written agreements were signed respectively. Location of exploration lines and boring holes were previously designed by the Preliminary Study Team but finally decided by this Study Team with minor changes due to local topographic conditions.

Physical properties measurement for soil investigation was also commissioned to a local contractor.

Chemical analysis of soil, water, dust etc, was undertaken by Tecamachalco Research Laboratory of CFM.

Actual survey works were advanced as illustrated in Fig.2-3 and 2-4. Table 2-1 shows total amount of the electric exploration and boring works in each survey area.

Detailed results obtained in each survey area are described in the following Chapters.

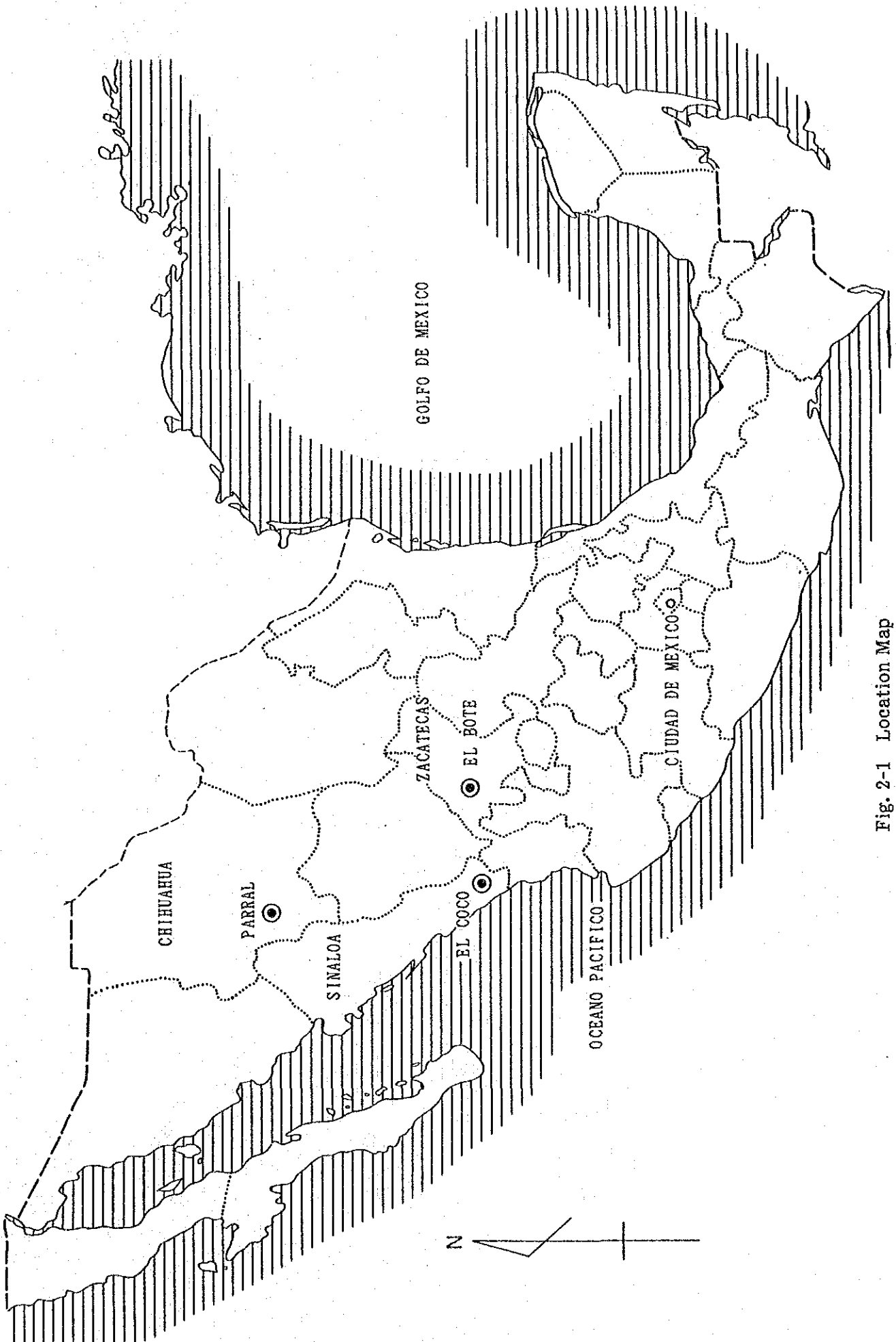


Fig. 2-1 Location Map



Fig. 2-2 Photographs of Survey Area (El Bote Tailing Dam) (1)



Fig. 2-2 Photographs of Survey Area (Parral Tailing Dam) (2)



Fig. 2-2 Photographs of Survey Area (New El Coco Planned Tailing Dam Site) (3)

	January, 1991			February			March		
	2nd decade	3rd	1st decade	2nd	3rd	1st decade	2nd	3rd	
Data Collection. Discussion etc.		---	---	---	---	---	---	---	
Elec. Exploration El Bote Parral New El Coco			---	---	---	---	---	---	
Boring Works El Bote Parral New El Coco			---	---	---	---	---	---	
Geo. Observation El Bote Parral New El Coco		---	---	---	---	---	---	---	
Measurements El Bote Parral New El Coco									
Remarks	1/21 Arrival in Mexico			3/6 Customs Cleared (Apparatus)			3/26 Leaving Mexico		

Fig. 2-3 Progress in the Field Investigation (Dry Season)

	J u l y , 1 9 9 1		A u g u s t			S e p t e m b e r			
	2nd decade	3rd	1st decade	2nd	3rd	1st decade	2nd	3rd	
Data Collection, Discussion etc.	—			—		—	—		
Clearing of Boring Hole El Bote Parral New El Coco		—	—		—				
Leveling El Bote Parral New El Coco		—		—	—				
Boring Works El Bote Parral New El Coco		—			—	—	—		
Geo. Observation El Bote Parral New El Coco		—		—	—	—	—		
Measurements El Bote Parral New El Coco		—		—	—	—	—		
Remarks	7/15 Arrival in Mexico						9/17 Leaving Mexico		

Fig. 2-4 Progress in the Field Investigation (Rainy Season)

Table 2-1 Total Amount of Electric Exploration and Boring Works

Survey Area	El Bote	Parral	New El Coco
Elec. Exploration (Dry Season)	49 stations	60 stations	26 stations
Boring Works (Dry Season)	No. Depth(m) Riverside B-1 10 B-2 30 B-3 20 <hr/> 3 60 Damsite D-1 29 D-2 19 D-3 15 <hr/> 3 63	No. Depth(m) Riverside B-1 10 B-2 15 B-3 40 <hr/> 3 65 Damsite D-1 17 D-2 12 <hr/> 2 29	No. Depth(m) Riverside B-1 50 B-2 105 B-3 20 B-4 30 B-5 14 B-6 10 B-7 14 B-8 14 <hr/> 8 257
Sub Total	6holes 123m	5holes 94m	8holes 257m
(Rainy Season)	NONE	Riverside B-4 15 Damsite D-3 17	Riverside B-9 20 B-10 15 B-11 15 B-12 15 B-13 10 <hr/> 5 75
Sub Total		2holes 32m	5holes 75m
TOTAL	6holes 123m	7holes 126m	13holes 332m

Remarks: Riverside borings were aimed at ground water movement but not always located in the vicinity of a river, while damsite borings were drilled in a tailing dam to study the property of soil. Refer to Location of the Drill Holes.

3. Survey Results and Countermeasures in the Area of El Bote

3. SURVEY RESULTS AND COUNTERMEASURES IN THE AREA OF EL BOTE

3.1 General Situation

3-1-1 Location, Topography and Climate

El Bote mine, one of the survey target, is located 2km northwest of Zacatecas, the capital city of the State of Zacatecas, in the central Mexico. It is about 2,400m above the sea level. The climate here is "Step type". Average temperature throughout a year is 10 ~ 15° C but goes down to 7° C in the winter season. The rainy season usually runs for five successive months starting in May till September, the rest of which is almost dry. Annual rainfall averages 660mm. Throughout the dry season the south-west wind blows so hard.

As to vegetation in this area, cactus and some shrubby plants like mulberry are mainly seen. On the downstream area from the mine, spreads an alluvial fan, which is being used as a pasture or a farm-land of corn, peas, red pepper and the like. In the north-west district, 10 ~ 15 km from the mine, are located several wells owned by the city authorities to supply service water to the city of Zacatecas.

3-1-2 Outline of the mine

El Bote mine was started by a private person in the late 19th century as a gold-silver-lead mine. Then, it was taken over by Bote Mining Co. in 1912, by Pittsburg Mining Co., U.S.A., in 1924 and then, by Carnegie Mining Co. in 1935. Since 1972, the entire operation has been unified by CFM as an organization, "Unidad Minero Metalurgica El Bote", and operated until now.

Total output from the underground mine reached 166,000 tons in 1989. According to recent records, metal contents in the crude ore are 0.8 g/t Au, 110 g/t Ag, 0.5% Pb and 1% Zn. Its mineral processing plant has a capacity of 650 tons a day, which is the highest among the whole plants owned by CFM. Up to 1987, lead and zinc concentrates had been recovered separately by differential flotation method, however, due to decrease in metal in the crude ore, it has been converted into bulk flotation for the recent four years to recover single sulfide bulk concentrate. In these days, when the metal contents are comparatively high, differential flotation is operated temporarily. In this case

about 600kg of sodium cyanide (NaCN) per month is added into flotation pulp to separate lead and zinc and this could bring water pollution problem of mine effluent. When bulk flotation is employed this harmful reagent is not used at all. Metal contents in the bulk concentrate are 20 g/t Au, 3,000 g/t Ag, 6% Pb and 12% Zn. Water consumption in the plant is about 1,400m³ a day, of which 1,000m³ is supplied as fresh water from the underground mine and the rest is recirculated from the tailing dam effluent. Waste materials discharged into nearby rivers without any treatment.

Tailing materials from the mineral processing and cyanidation plants are now being deposited with upstream depositing method in the tailing dam, situated on the opposite side of the valley. The height of the dam is over 40m with average slope of 45°. The north-western part of the dam has already been piled and now the south-western part is being filled. The tailing material is classified with cyclones, of which underflow, coarse and medium sized sands are discharged into the central part.

On the embankment slope of the dam, a lilly-shaped crevice showing outflow of deposited sand is clearly seen. Any countermeasures are urgently required.

3-2 Geology

3-2-1 Outline of geology

El Bote Mine in the survey area is located near Zacatecas, Capital of Zacatecas State, on the western slope of the Sierra Madre Occidental. A large scale Caldera structure is recognized in the area of the south of Zacatecas and the northern end of the structure is cut by La Cantera Fault which extends from east to west. The survey area is located at the north of La Cantera Fault, where the La Cantera Vein lays in NW-SE direction.

The basement in the survey area mainly consists of Triassic Pimienta metasediments. The metasediments is covered by Eocene andesite of Tertiary age. La Cantera Vein and rhyolite dykes intruded into these rocks. La Cantera Veins developed are caused by tension fracture accompanied with arching of early stage of the caldera forming Post Eocene, and after, the Vein was deformed and enlarged by the movement of gravity fault. In the survey area, La Cantera Vein is the biggest and the most economically important vein deposits, which is rich in silver. In the Pleistocene period, the fans developed along the western foot

of Sierra Madere Occidental by the erosion of the mountains, and recently Terrace has formed along the rivers.

3-2-2 Geology and geological structure

Geological interpretation by aerial photographs, field reconnaissance and drilling works were carried out in order to clarify the geology of El Bote area. As the result of the survey, it was confirmed that the basement of this area is Pimienta metasediments of Triassic and the layer represents about 60% of the whole site, shown in Fig.3-2-1,3-2-2 and 3-2-3. The Pimienta metasediments show irregular direction both the strikes and dips because of the complex structure of folding. However, the observation that the dip of the layer generally inclines NE to E or SE except the area of western end indicates the lower layer is distributed in the western area and upper layer in the eastern area, respectively. The basement rocks, as called metasediments, was generally affected by low grade metamorphism. Metamorphic rocks, mainly composed of phyllites, widely distributes in central and northern part of the area.

The Eocene andesites of Tertiary distribute covering unconformably the basement in the south-eastern part of this area. The strike of NW-SE and the strike of NE direction are considered to be dominant in the andesite.

The rhyolite dykes of post Eocene and the ore veins, prominent as La Cantera Vein and closely related with the rhyolite dykes, have the direction of WNW-ESE and occur as belt type distribution crossing the northern part of El Bote tailing dam. The Quarternary old fan deposits form flat plane in the north-western and central part of this area. Recent terrace deposits develop along the river by erosion of the old fan deposits.

The Pimienta metasediments forming the basement was structurally affected by folding. The possibility of existence of an anticline axis near the drilling hole B-1 with NNE-SSW direction is high (Fig.3-2-4). The dips and strikes markedly change bordering the area near B-1 hole (Fig.3-2-1,3-2-2, and 3-2-5).

Fig.3-2-6 shows fracture survey sites. Fig.3-2-7 shows Wulff's net of fracture directions. From this survey, it is also considered that there are faults with three different directions. One type is NW-SE stretched parallel to the direction of that of the La Candera Vein mentioned before. This fault is considered to be formed by tension fracture following the formation of the

Caldera structure in the southern part of the area. Other two types of faults have approximately NE-SW and ENE-WSW direction to cut the vein. Their strikes are approximately parallel to the strike of the basement. However, the nature of them is unknown.

(1) Triassic system (Pimienta metasediments)

The Triassic System in the area named Pimienta metasediments is composed of phyllite, sericite schist, limestone, quartzite and slate.

① Phyllite

The phyllite shows grayish white color and extremely fragile by weathering. The rocks are very stratified and laminable or fissile. The distributed area is biggest in the system and occupied the northern and the central area. Dips and strikes are irregular by generally remarkable folding.

② Sericite schist

The genesis of the sericite schist in this area is originated from alteration of phyllite to yield the small amount of sericite. It shows white or grayish white color and be remarkably fragile. The distribution is in the northern part of El Bote tailing dam and is partly recognized along the vein.

③ Limestone

The limestone shows dark grayish color, and hard and dense. The rock generally has the foliation structure in muddy part, showing zonal distribution within both two strata in the south-western part of El Bote mineral processing plant. The traces of an old stope remains on the slope of the hillside of the south-western part of the area.

④ Quartzite

The quartzite distributes in south-eastern part of the El Bote mineral processing plant showing zonal distribution south to north direction. It is considered to be formed by the same metamorphic process of phyllites from sandy rocks.

⑤ Slate

The slate exists in the uppermost and lower layer of the Triassic system. The distribution is in south-eastern and western area near El Bote plant. The distributed area in the western part is particularly large and the occurrence was confirmed by the three drilling holes for the observation of groundwater located in the west of anticline axis. By the observation of drilling cores, comparably fresh part of the slate shows black, but, in weathering part it shows gray to brownish color.

The lamina is remarkably developed and calcite veins are crystallized and easily crushed along the lamina. The strike and dip of this layer are not constant due to the small folding (intraformational folding). However, the strike and dip are approximately $N45 \sim 55^\circ W$ and $10 \sim 40^\circ NE$, respectively, in the western part of B-1 drilling hole. On the other hand, the strike and dip are $N40 \sim 70^\circ E$ and $20 \sim 40^\circ SE$ in the eastern part, respectively. Judging from this observation, the anticline axis is presumed to exist near B-1 drilling hole.

(2) Tertiary System

The Tertiary System is composed of andesite of Eocene, rhyolite dykes and ore veins of post Eocene. This has not been confirmed by drilling, however, recognized by the survey of surface and mine.

① Andesite

The andesite is altered and shows dark greenish to dark greenish gray color. The distribution of the andesites is in the south-eastern part of the area and covers the basement unconformably. The rhyolite dykes mentioned later intrude into this andesite layer.

② Rhyolite dyke

The dyke rock is hard, dense, and greenish white to pale yellowish white rhyolite. The dykes consist of many rock veins intruding into the andesite of Eocene and show WNW-ESE direction in the central part of the area. The distribution is clearly recognized through the aerial photographs. The dykes are exposed near the tops of the hills to form the ridges located north of El Bote plant.

③ Veins

The geological map of the ore vein has been made by El Bote Mine. The age of the mineralization was mentioned already. The vein system occurred in the concentric circle with same center of the Caldera during the Caldera forming process and located in the southern part of the area with $N45^{\circ} \sim 85^{\circ} W$ of the strike and $50^{\circ} \sim 70^{\circ} SW$ or $75^{\circ} NE$ of the dip. The vein system includes Au, Ag, Pb, Zn, Cu and economically most important in this area.

(3) Quarternary system

The Quaternary system is composed of old fan deposits of Pleistocene, the terrace deposits of Holocene and recent talus deposits.

① Old fan deposits

The deposits form the gently flat plane in the central and north-western part of the area. The deposits are mainly composed of poorly sorted sands and gravels with large amount of angular gravels of Pimienta metasediments and rhyolite.

② Terrace deposits

The deposits distribute along the present river and are confirmed at all the drilling holes of B-1, B-2 and B-3 for the observation of groundwater. The existence of the deposits in the B-1 drilling hole located upstream side from GL. -2.80 to 8.60m in depth, and the occurrence is gravel bed, fine grained-sand bed, medium grained sand bed, fine-grained sand bed, and medium to fine-grained sand bed from lower part to upper part. The deposits in the B-2 hole in mid-stream, exist in GL -2.00 to 8.00m in depth, and the occurrence in B-2 hole is gravel bed, fine grained-sand bed, very fine-grained sand bed from lower part to upper part. The occurrence in B-3 hole located in downstream is silt bed with gravel in GL. 0.20 to 5.10m in depth. The sorting of the grains in the sand beds develops well in the lower stream side than in the upper stream side.

③ Recent talus deposits

These deposits are composed of sands and gravels deposited in the present

river bed with the round to subangular gravels of the basement rocks, acidic rocks and andesite.

3-3 Electrical Prospecting

3-3-1 Method of Survey

The purpose of electrical prospecting was to examine the underground resistivity. The Schlumberger's Electrode Array was used in this survey. This method uses the four electrode arrangement in resistivity Vertical Electrical Sounding (VES). Schinterx Model IPC7 (2.5KW) was used in this prospect and its maximum AB spacing of AMNB electrode system is 400m .

The survey was carried out with 49 stations arranged on 20 lines. The location of the stations is shown in Fig.3-3-1. Data of the survey were processed to analyse resistivity with the software for analysis (RESIX PLUS DC).

3-3-2 Results of Survey

The analysed resistivity is classified into following four groups and is shown in Fig.3-3-2.

S Zone: tens to thousands of $\Omega \cdot m$

L Zone: Less than 100 $\Omega \cdot m$

M Zone: 100 ~ 200 $\Omega \cdot m$

H Zone: more than 200 $\Omega \cdot m$

L zone shows low resistivity, M zone shows medium resistivity, H zone shows high resistivity and S zone shows complex zone of low and high resistivity.

S zone forms the surface in thickness of 5m ~ 45m, the average thickness is 20m. S zone is composed of the recent terrace deposits (Holocene of Quarternary), old fan deposits and weathered overburden of phyllites, slates and limestones of Triassic System.

M zone and H zone forms in the eastern part of 9-39-27 line and the lower part of S zone. There are less L zones in the eastern part of this line. But, M zone (Medium resistivity) or H zone (High resistivity zone) is formed in the lower part than 150m of S zone.

M zone and H zone are composed of phyllite and limestone of Triassic System. Almost all the part of H zone corresponds to the part lying between Triassic

System. M zone and H zone correspond to the part of the axis of anticline and the eastern wing of the anticline from the geological structure.

Ground water movement was observed in S zone and L zone in boring test. From this fact, It is considered that S zone and L zone are aquifer. M zone is aquitard and H zone is aquiclude or aquifuge, respectively.

3-4 Hydrology

The water system of the survey area is shown in Fig.3-4-1. The El Bote River flows down through the southern part of the mineral processing plant from the ESE to WNW. The purpose of the survey is to examine the effect of the waste water from the tailing dam on surface and groundwater. The collection of flow data and various analysis of water were carried out at the points shown in Fig. 3-4-1 both in the dry and the rainy season.

3-4-1 The Surface Water

The flow rate of the rivers in the survey area is generally small throughout the year. The branch was particularly dried up in the dry season. Survey of the rate of streamflow and analysis of water quality were carried out at the points shown below both in the dry and the rainy season.

In the dry season, sampling sites for streamflow are No.1 ~ No.6, and for water quality are B-D1 and B-R1 ~ R5.

In the rainy season, sampling site for streamflow are No.0 ~ No.6, and for water quality are B-D1, B-W1 and B-R1 ~ R7.

(1) The flow rate of surface water

The measurement of current velocity by Price flow meter and calculation of the rate of streamflow (cross-sectional area of flow) was carried out at No.0 ~ No.6. The results are shown in Table 3-4-1. Fig.3-4-2 shows modified chart of the flow rate on 20, March in the dry season and on 12 to 13, August in the rainy season.

From Fig.3-4-2, the variation in the streamflow rate is large in the sections between No.1 ~ No.4, No.4 ~ No.5 and No.5 ~ No.6 in the dry season. In the rainy season, the variation of the flow rate is large in the stream between No.0 ~ No.1 and No.5 ~ No.6. The reason of these phenomena is presumed as following;

① Variation of streamflow in the dry season

i) Increase in the flow rate between the points No.1 and No.4

It is estimated that the flow rate at point 4(1,213.1 m³/day) is derived from the addition of the Talamantes River(880.4 m³/day) to the main stream of the El Bote River at point 1. Therefore, it is presumed that the flow rate of the main stream of El Bote River is approximately 330m³/day. The waste water from the Parral plant flows into the El Bote River in this point of the river.

ii) Decrease in the flow rate between the points No.4 and No.5

In this section of the river, the flow rate amount, 1,213.1m³/day at point 4, decreases down to 572.0m³/day at point 5. About 640m³/day has disappeared, because weathered slate is exposed on the bank of the river at both points, thickness of the river deposits is thought to be almost constant. And, also the effect of evaporation is negligible in this short range. There are only two houses in this section. So, the decrease in the water is not by their home uses. These facts indicate there might be another reason of disappearance of water of about 640m³/day in this section of 0.5km. The surface water is considered to make not only underflow to the river deposits but also rapid seepage to underground.

The geological structure and the result of electrical prospecting indicate that there is an axis of anticline around point No.4, and the river cuts across the axis of anticline and flows to the west guided by the inclination of the layer(Fig.3-4-1). And low resistivity (less than 100 $\Omega \cdot m$) zone spreads out to the west into deeper area. These facts indicate that the surface water easily penetrates to underground in the western side from point No.4, and it is considered that this may be the most realistic reason of the river water penetration.

iii) Decrease of the flow rate between the points No.5 and No.6

The decreasing amount of the flow is only 160m³/day. The amount is considered by the penetration of the river water into underground, because of the geological environment in this section is almost the same as the section of the area of the lower reaches from No.4. The amount of penetration is less than that of the upper reach's section, because of decreasing cracks in the far

distance of the folding axis.

② Variation in the flow rate in the rainy season

i) Increase in the flow rate between the points No.0 and No.1

Increased amount of $447.3\text{m}^3/\text{day}$ at point No.1 is estimated to be derived from a big branch of the river in this area and flow of waste water from the mine into the river.

ii) Decrease in the flow rate between the points No.5 ~ No.6

The $1,212.3\text{m}^3/\text{day}$ of the flow at point No.5 decreases to $464.2\text{m}^3/\text{day}$ at point No.6. Approximately $759\text{m}^3/\text{day}$ of the flow disappears in this section. The flow also decreases in the the dry season. Developing cracks due to the folding are considered to be the main cause of the decrease of the flow.

③ The Variation in the flow volume in the dry and the rainy season

The variation of the flow volume is generally small in the survey area. The flow volume in the dry and the rainy season are approximately the same at points No.4 and No.6 and others.

Compared with the data of the dry season and that of the rainy season in upper reaches, the flow at point No.1 is approximately twice of that in the rainy season. Each fact seems to be contradictory from the seasonal characteristics. But, the waste water from the mine flows into between No.1 and No.2 and the variation in the flow volume in this section is more affected by this variation than the seasonal change. The flow at No.2 and No.3 are affected by the difference of the amount of evaporation. The flow volume in the dry and the rainy season are nearly the same. The seasonal change can not be recognized in this section.

(2) Water quality of the surface water

The sampling of the surface water was carried out at the 9 points of B-D1, B-W1 and B-R1 ~ B-R7 in order to analyse pH and pollutants. The analysis data of the samples of surface water are shown in Table 3-4-3. Background and water supply ceiling of pollutants are shown in Table 3-4-2. The results of chemical analysis are shown in Fig.3-4-3.

① Background contamination

Point B-R6 is located in the uppermost reaches in the site, is not affected by CFM mineral processing plant and private plant. But, as the area and its environs are widely affected by natural mineralization, the water includes Cu, Pb, Zn, Fe, As and Cd. The background in this area is obviously contaminated and no connection with the existing plant. Particularly, the contents of Fe and Cd exceed the upper limit of the Environmental Standard of Pollutant Content all over the area, so the river water in the area is not good for drinking.

The area including point B-R7 has the same tendency except As content.

② B-R2 contamination

It is necessary to pay attention to the analysis data of B-R2 sample. The results of analysis of the water from point B-R2 shows extremely high content of pollutants such as Cu, Pb, Fe, Cd, Total Cr and As, and shows abnormally high content compared with that of the water at the other points.

The point is located along the branch at upper reaches of CFM tailing dam and within the distribution area of ore veins. The private mine is located in the upper reaches than this point. There are many bounding stones with including ore piling to as thick bed in the riverbed. River water flows trickling in the rainy season. In the dry season, water is little showing yellowish orange color, and is stagnant. Sulphate minerals crystallize in the bank and on the riverbed. Compared with chemical analysis data of water in the dry season and in the rainy season, the content of pollutants concentrate in the dry season. The concentration of pollutants is due to scarce rain fall and increased evaporation.

Therefore, the extreme pollution of the water at point B-R2 is mainly caused by the distribution of vein near surface and little from the slime and waste water from the private mine located in the upper reaches.

③ Contamination near CFM processing plant

The sample at B-W1 is the waste water discharged from CFM plant to a settling pond. The content of pollutants is shown in Table 3-4-3. The contents of Pb, Fe, Cd and Total Cr exceed the upper limit of the Environmental Standard of Pollutants Content. The settling pond into which the waste water is flowing is

located just the lower reaches of the tailing dam which was constructed using topographical features of El Bote River. The contents of pollutants (Pb, Fe, Cd and Total Cr) exceed the upper limit of the Environmental Standard Pollutants Content all through the season. It suggests that pollution by Zn is mainly caused by the material supplied from the upper reaches. It is obvious that the origin of pollution is the mine water from point B-M2 (San Bartolo Mine) which is discharged to the upper reaches of settling pond.

④ Contamination between B-R6 and B-R1

Point B-R1 locates in the lower reaches of B-R6 but in the upper reaches of CMF plant, therefore, B-R1 is not affected by the dressing plant. By the surface water analysis of this area, the contents of Fe and Cd exceed the upper limit of the Environmental Standard in the dry season. Addition to the Fe and Cd content, the content of Pb also exceeds the upper limit of the Environmental Standard in the rainy season. The waste water discharged from Purisima Mine, which locates between B-R6 and B-R1 makes the water quality worse. By the analysis data of the mine water of Purisima Mine (near B-M1), the contents of Pb, Fe and Cd exceed the upper limit of the Environmental Standard. As regard to the content of Pb, the waste water discharged from the mine is obviously responsible. B-R1 point is the same point as No.1 described in the Fig.3-4-1. The change in the flow rate is considered to be affected by the change of the discharging rate and discharging time from the mine, and the measurement time as well. It is less affected by seasonal change. Therefore, the water quality at the point is considered to be affected by the change of mixing ratio of the amount of waste water from the mine and surface water from the upper reaches, and sampling time of the water.

⑤ Contamination between B-R3 and B-R5

In the section between B-R3 and B-R5, the contents of Pb, Zn, Fe and Cd exceed the upper limit of the Environmental Standard in the dry season. In the rainy season, only Fe and Cd exceed the limit of the Environmental Standard. Judging from the analysis data (Table3-4-3), the background contents of Fe and Cd exceed the limit of the Environmental Standard, the content of pollutants is considered to show the general characteristics of the area due to precipitation,

which dilute the local characteristics in the rainy season. On the other hand, it is presumed to occur the concentration of the pollutants due to the marked decline of precipitation and increase of evaporation. As the result, the contents of Pb and Zn are considered to exceed the upper limit of the Environmental Standard reflecting local pollution.

⑥ Summary

The number of origins of the pollution of the survey site is considered to be three mineralization zone near B-R2, the settling pond of the CMF plant and the outlet of waste water of Prisima Mine. However, the mine water of Prisima includes Zn 1.7 %, which is less than that of surface water of this site (B-R1 ~ B-R7). The water from the mine hardly affects the pollution of the area of the lower reaches. Therefore, the biggest origin of the pollution is the mineralization area near B-R2. The slime and waste water from the mine in the upper reaches of the area gives some influence on the pollution. There are some possibilities that penetrating water from the settling pond gives some influence on the pollution.

pH of the waste water from the dressing plant and river water except the sample at B-R2 is in the range of 7.50 ~ 8.20, which is weakly alkaline. However, the sample of B-R2 shows strong acidity of pH 2.55. From the facts, B-R2 area is obviously recognized to be markedly polluted.

3-4-2 Groundwater

Electric prospecting and survey of the streamflow (current speed) with three observation holes, and analysis of water quality of the observation holes and underground mine were carried out in order to examine the influence of waste water from CFM plant and the tailing dam on groundwater.

(1) The flow rate of groundwater

The survey of the flow rate (current speed) and the position of aquiferous layer was carried out in three observation holes along the El Bote River, just the lower reaches of the tailing dam. The strainer tubes made by vinyl chloride of 50mm of inside diameter were inserted in the drilling holes. Current speed was measured using micro flow meter. The results are shown in Table 3-4-4, Fig. 3-4-4,

and Fig.3-4-6. In B-1 hole, because of very weak current, aquiferous layer could not be confirmed. In B-2 hole, the aquiferous layer was recognized in 2 strata of EL 2,308 ~ 2,310m and EL 2,315 ~ 2,320 m, respectively. In B-3 hole, aquiferous layer was recognized in EL 2,302 ~ 2,314m.

The equivalent-resistivity plans of the depth of approximately EL.2,310m and EL.2,320m by the resistivity of underground are shown in Fig.3-4-5. The plan shows that both B-1 and B-2 are located in the low resistivity zone of less than $100 \Omega \cdot m$. It is presumed that the existence of the fault from the shape of iso-resistivity line of $150 \Omega \cdot m$ and $200 \Omega \cdot m$, and also considered to exist groundwater along the fault. The aquiferous layer exists within slate, it may be slightly different from shale of Parral, permeable layer exists in the resistivity zone at least less than $150 \Omega \cdot m$ in Parral area. According to the resistivity in Parral, the permeable layer is considered to exist in the zone less than $150 \Omega \cdot m$ of resistivity. The current direction of groundwater is considered to WNW along the low resistivity zone. The review of the survey is shown in Table 3-4-5.

According to Table 3-4-5, the flow rate of the lower aquiferous layer in B-2 hole is approximately $430,000 \sim 560,000 \text{ m}^3/\text{day}$, and that of the upper layer is $170,000 \sim 310,000 \text{ m}^3/\text{day}$. However, the measurement value in B-2 shown in Fig.3-4-6, as the location of B-2 is nearly the edge of the low resistivity zone, it is possible that the whole flow rate in low resistivity zone is less than the average flow rate of groundwater. It can be estimated by the fact that the flow rate of the hole of B-3 is larger than in B-2 which locates in the upper reaches.

The current speed of groundwater generally increases in rainy season. The groundwater level also rises approximately 0.6m in B-1 and B-2, and approximately 0.8m in B-3 in the rainy season compared with the dry season. By the fact, the groundwater in shallow place along the El Bote River occur to change of the flow rate reflecting seasonal change.

(2) Water quality of the ground water

The water samples are collected at 6 holes of B-B1 ~ B-B3 and B-M1 ~ B-M3 in order to analyse water quality including measurement of pH. The result is shown in Table 3-4-6.

Considering the result shown in Table 3-4-6, there is slight difference

between B-M1 ~ B-M3 which were sampled in mineralized zone and B-B1 ~ B-B3 in shallow bed along the river. The contents of Pb, Fe and Cd of the mine water of B-M1 ~ B-M3 exceed the upper limit of the Environmental Standard. On the other hand, the content of Cd in B-B1 ~ B-B3 decreases and the contents of Pb and Fe exceed the upper limit of the Environment Standard. The contents of Cu, Pb and Total Cr in B-B1 ~ B-B3 along the river increase in the dry season, and Zn, Cd and Hg were detected in wet season. It is considered to be caused of the fluctuation of groundwater level and the flow rate, or the vertical and horizontal change of the stream flow, and permeable layer is presumed to slightly differ in the dry and the rainy season.

Therefore, the groundwater in shallow bed along the river fluctuates not only in the flow rate but also in water quality affected by seasonal change. The content of almost all the pollutants in the sample at B-M2 which is the mine water of San Bartolo Mine is higher than that of other groundwater samples. Particularly, the content of Zn shows abnormally high value of 140 ppm. Moreover, pH is lowest different from other samples that show almost neutrality.

Almost all the waste water from CFM mineral processing plant flows into the settling pond located just below the plant. The contents of Pb, Zn, Fe, Cd and total Cr of the sample at B-D1 in settling pond exceed the upper limit of the Environmental Standard. However, in the lower reaches of the plant only Pb and Fe exceed the upper limit of the Environmental Standard. Therefore, it is not considered that the penetrating water from the plant is the major origin of the pollution of groundwater which exists in the lower reaches.

3-4-3 Groundwater Flow System Simulation

Optimum simulation blocks of physical and hydraulic properties are modelled around El Bote Mine. A Groundwater flow system is simulated by these properties which are obtained by integrating the results of meteorological, geological, hydrological surveys and soil test.

By this simulation, clarified are water table, flow direction and flow speed. Simulation results are contributed to calculate effective groundwater harness, waste water recycle and mining pollutant dispersion.

(1) Simulation Method

A numerical simulation for groundwater flow is conducted by the use of three dimension simulator "GWS3D2P" originally developed by Dr. Hiroyuki Tosaka of Tokyo University. In this simulator, Darcy's law and mass balance equations are analysed by Finite Difference Method. The details of this simulator is described in Appendix A "Numerical Simulation Technology for Subsurface Fluid Flow".

(2) Simulation Model

① Block Model

Simulation area is rectangular, 15km wide in the NW direction and 12km wide in the NE direction (Fig.3-4-8). El Bote Mine is located in the southeastern side of the area. The veins and fissures generally strike northwest around El Bote ore deposits. The water supply pump of Zacatecas municipality is located on the northwestern side of the area. The simulation is conducted to predict the pollutant dispersion from El Bote mine to the municipality water supply pump. Consequently, the direction of the simulation area is in accordance with the vein strike, and the area is decided to cover the mine and the pump site. The simulation depth is decided to 1,800m above sea level, because of the pumping 200m below the surface at the municipality water supply site and the pumping 150m below the surface at El Bote mine site.

The simulation area is divided into 30 blocks in the northwest direction, 31 blocks in the northeast direction. The block size is 200m × 200m wide around El Bote mine, 1.2km × 1.2km wide around the marginal area. X and Y axes are in the directions of NW-SE and NE-SW, respectively in the figure.

Vertically, the area is divided into 9 underground layers and 1 atmosphere layer, total 10 layers. The uppermost atmosphere layer is the first layer Z1. Surface layers are 10 to 20m thick, deep site layers are 200m thick. The height of each block is represented by the elevation of the center of the block as Fig.3-4-9 shows.

② Permeability and Porosity Model

Permeability and porosity of each simulation block are determined by integrating the geological, geophysical and hydraulic properties.

Geologically, the mountain side, in which El Bote mine is situated, is

underlain by compact Triassic and Tertiary rocks which are not permeable. On the other hand, the hill side is underlain by thick alluvial deposits which are permeable. Triassic rocks of hill side is assumed to be situated 1,900m above sea level, which rocks is situated in deeper site than the rocks of mountain side.

The fissures and veins around El Bote Mine generally strike in the NW and NE directions. Therefore, The rocks which accompany fissures or veins are permeable in this direction. The mountain side is upheaved in the N-S direction and the permeable fissures parallel to this direction are also recognized in the boundary between mountain side and hill side.

As the results of the electrical prospecting and boring observation, low resistivity zone and low-high complex resistivity zone correspond to aquifer. Intermediate resistivity zone corresponds to aquitard. High resistivity zone corresponds to aquiclude and aquifuge.

As compared with geology and geological structure, the aquifer zone is equivalent to alluvial deposit and the Triassic-terrace deposit boundary and fault zone. The aquitard is equivalent to weathered overburden and fault periphery. The aquiclude is equivalent to surface soil and clayey terrace deposit. The aquifuge is equivalent to the Triassic of mountain side.

As the results (Table 3-4-7) of grain size distribution, the aquifer permeability coefficient of alluvial sandy deposits is 10^{-2} cm/sec (sample No. BR-1,2). The aquiclude permeability coefficient of clayey terrace deposit is $10^{-5} \sim 10^{-6}$ cm/sec (BR-3,4,5). Consequently, the aquifer permeability coefficient of alluvial sandy to clayey deposits is set to 5×10^{-4} cm/sec. The aquiclude's is 10^{-5} cm/sec. The aquitard's is 10^{-4} cm/sec. The aquifuge's is 10^{-7} cm/sec.

At El Bote mine, several big veins are embedded. The veins have been mined 3 km long along the strikes, 400m wide and 200m deep below the surface. So, the permeability coefficient of the vein zone is presumed to be 10^{-3} cm/sec, because the vein zone corresponds to big fault zone.

Porosity is presumed to be 30% to vein and aquifer, 20% to aquitard, 15% to aquiclude, 5% to aquifuge, respectively.

Table 3-4-8 shows permeability and porosity model. On the basis of this table, Fig.3-4-9 shows rock classification. In this plane map (X-Y CROSS SECTIONAL VIEW), the coordinates of left-bottom and right-top ends are (X1,Y1) and (X30,Y31), respectively. In the cross section (Y-Z CROSS SECTIONAL VIEW), left

and right ends are Y31 and Y1, respectively. The legend No. of Table 3-4-8 corresponds to it of Fig.3-4-9.

③ Hydraulic Model

El Bote river flow down northwestward near El Bote mine. As Fig.3-4-1 shows, No.4 river flow measuring point is situated downstream from El Bote mine. At this No.4 point, flow rate is constant through dry and rainy season. On the other hand, upstream from this point, the river is divided into tributary streams which are not constant flow rate. Therefore, the flow rate $1,200 \text{ m}^3/\text{day}$ is set at No.4 point for simulation.

Each Water level of the observation wells is set for simulation as to be situated at the top of the third layer counted from atmosphere layer. However, the water level at El Bote mine is set at the top of of the seventh layer because of pumping water from the mine tunnel which is 200m below the surface.

④ Meteorological Model

Annual precipitation is 400mm on the average. 95 percent of it precipitate during rainy season from May to September. Therefore, during 5 months, the precipitation is 380mm from May to September. During other 7 months the precipitation is 20mm.

Evaporation data are referred from New El Coco observation. Evaporation of it ranges 0.35 to 0.84mm/day.

Recharge rate is set as 0mm/day during dry season, 2mm/day during rainy season, by precipitation minus evaporation.

⑤ Recharge Discharge Model

Groundwater of El Bote mine is pumped 200m below the surface at the rate of $1,200 \text{ m}^3/\text{day}$. The municipality well pumps 200m below the surface at the rate of $1,000 \text{ m}^3/\text{day}$. The mineral dressing plant of El Bote mine discharges waste water at the rate of $1,000 \text{ m}^3/\text{day}$.

These coordinates are (X1,Y29), (X26,Y12), (X24,Y11), respectively.

(3) Simulation Results

Fig.3-4-10 shows groundwater saturation maps. Rainy season map is of the 150th

day, counted from the first day of rainy season. Dry season map is of the 360th day, which is end of dry season, counted from the first day of rainy season. In this maps, blue color zone is saturated with free water. In accordance with the changing blue to yellow, the saturation level decreases.

The alluvial deposits area (A site) shows high saturation degrees of the surface layers in rainy season compared with dry season. The mountain side (B site) show same saturation degrees in both rainy and dry seasons. This means not remarkable change of groundwater level ,but change of saturation degrees above the groundwater level. This difference of saturation is attributed to the small water level variation in both seasons.

Therefore, there is a strong suspicion that pollutants are stored in the surface layer, because the groundwater including eventwater moves in the top thin layer in the aquifer, under the variable depth of water table.

100% saturated zone is widely distributed in the surface layers on the C and D side ,compared with A side . El Bote Mine is located at weakly saturated zone of Site E, from which groundwater is pumped.

Influence of the El Bote river flow is clearly recognized down to the G site , below to the second and third layers ,and weakly to the fourth layer. The influence range is 7km west from the El Bote Mine, 2.5km wide, 80m deep.

The waste water the El Bote mine is discharged at the rate of $1,000\text{m}^3/\text{day}$. Flow rate of the El Bote river is $1,200\text{m}^3/\text{day}$. Most of the flow is attributed to the waste water discharge. From the results of chemical water analysis, Water pollution is attributed to mineralization zone or the discharge from the other mines rather than El Bote Mine.

In either case, the contaminated water infiltrates down to the alluvial area (hill side). To prevent this infiltration, pollutants extraction and waste water recycle should be conducted not so as to discharge the waste water into El Bote river.

Fig.3-4-11 shows groundwater velocity plane and cross sectional maps. Rainy season map is of the 150th day, counted from the first day of rainy season. Dry season map is of the 360th day, which is end of dry season, counted from the first day of rainy season. The velocity is presented by X, Y, and Z components, that is NW-SE, NE-SW, and vertical directions, respectively. The length of segments is proportioned to the velocity.

The seventh layer maps of rainy season (the 150th day) indicates clear flow direction to the El Bote mine tunnel(E site). In the alluvial area (A), the velocity of Y component is remarkably larger than of X component. This indicates that the groundwater flows south-westward, because this flow direction is caused by the potential inclination from north-eastern mountain side to south-western alluvial hill side. The velocity of the dry season is weakly slower ,but has the same direction as the rainy season.

The municipal water well is situated at the site F on the map. Not observed the flow direction from El Bote mine to this site, because above-mentioned potential inclination prevents the flow direction from the El Bote mine to this well. Judging from this simulation, the direct influence of the waste water of El Bote mine is not considerable.

It is easy to estimate that polluted groundwater flows to the well faster than present rate of groundwater flow from mountain side to hill side, if pumping up too much groundwater to keep the balance of the groundwater potential distributions of present, for example, people needs much amounts of water for drinking and for industries in the Zacatecas city.

We certainly propose, therefore, to make a observation system of groundwater to know the behavior of polluted groundwater from the mining area. The cross section maps of the groundwater velocity show the down-flow in the surface layers, the up-flow in the deep layers, and lateral flow in apart from the mine. This lateral flow is rapid in the surface layers.

3-5 Soil

Accompanied with mining activities, some harmful metal elements are transported as ions after dissolving into rain and groundwater, or carried away as dust by the wind. Both transportation result in the accumulation of these elements in the soil. To know the present situation,14 soil samples were taken for chemical analysis of the 9 elements, Cu,Pb, Zn, Fe, Cd, Sb, Cr, As, and Hg.

3-5-1 Assay results

Fig.3-5-1 shows the soil sampling map in and around the mine site. These assay results are given in Table3-5-1.

(1) Cu

Higher level of copper content, 220 and 470ppm, are detected in the samples BS-2 and BS-3 respectively. These were taken at nearest points to the CFM tailing dam. Samples, BS-1, BS-1, BS-B3, and BS-B5, taken from the south-eastern part from these points also show the high contents over 100ppm. On the other hand, samples, BS-B8, BS-4, and BS-B7 taken from the west of the dam, show lower levels of 37, 33, and 88ppm, respectively.

(2) Pb

Samples, BS-2, BS-B2, and BS-B4 contain the higher levels of 1,400, 1,000, and 530ppm respectively. Samples, BS-B1, BS-1, and BS-2 also show high levels of 840, 740, and 560ppm. These values form a highly contaminated zone around the dam.

(3) Zn

Samples, BS-1, BS-2, BS-3, BS-B1, BS-B2 and BS-B4, contain higher levels of 1,900, 3,200, 940, 4,200, 1,900, and 740ppm respectively. These form a highly contaminated zone around the dam. Other samples show the values between 100 ~ 300ppm.

(4) Fe

Samples, BS-B3, BS-B5 and BS-B6 contain higher levels of 7.5, 8.3, and 6.7% respectively, while the others are under 5%.

(5) Cd

BS-B1 shows the highest level of 44ppm. Also BS-2 and BS-B2 in the environs contain the high level of 26 and 19ppm, however, unlike the other elements no markedly contaminated zone is seen.

(6) Sb

All the values analyzed are between 20 ~ 70ppm. The highest is 68ppm of BS-B6, while the lowest is 20ppm of BS-1.

(7) As

Samples, BS-1 and BS-2 contain the higher levels of 120 and 190ppm. Others distribute in the range between 7 ~ 74ppm. A highly contaminated zone is seen around the dam but not so high as Cu, Pb and Zn.

(8) Hg

The highest value is 3.4 ppm of sample BS-B1.

3-5-2 Results and discussion

As the results of the soil assay in El Bote area, some extraordinarily high level of contamination were detected except Fe and Cr. Especially, around the tailing dam, concentration of Cu, Pb and Zn is remarkable.

In this concentration zone the ratio of Cu:Pb:Zn is not always constant and this suggests that the contamination is not brought from any single source but from diversified sources like geological features or natural mineralization, dust particles carried from the dam and effluents of the mining activities.

In the samples of BS-4, BS-7 and BS-8, taken from the west of the dam, each metal content is lower than the others. Since this region is not affected by dust, mineralization and other geological features, these levels of metal content supposedly represent the average in the Quaternary Sediments.

3-6 Tailing Dam

3-6-1 Purpose of the survey

The purposes of survey of the tailing dam are as follows;

- (1) To study the drainage conditions of the tailing dam in the rainy season in order to make the practical counter plan of the waste water drainage.
- (2) To carry out soil tests of the banking materials of the tailing dam in order to study their characteristics and to evaluate the stability of the dam based on the characteristics of the material.
- (3) To study the possible outflow of soil in rainy weather and to examine the proper counterplan.

3-6-2 Outline of the survey

(1) The survey of present situation of the tailing dam

① Drainage condition of the tailing dam in rainy weather

② Outflow of soil in rainy weather

(2) Observation of water level (Phreatic line measurement in the tailing dam)

(3) Sampling of undisturbed cores in order to make laboratory soil tests

(4) Laboratory soil tests

(5) Measurement of cross section of the tailing dam

(6) Levelling

(7) Environmental study

Collection of meteorological data (precipitation, wind direction, wind speed, etc.)

3-6-3 Results of the survey

(1) Present situation of the tailing dam

There is no surface water in El Bote Tailing dam, because the dam is unused now. Rain water partly infiltrates into the dam and others overflows as surface water. The paths of surface water is shown in Fig.3-6-1. The surface water of the first dam flows through the big lillytrench of the central part of the bank into the second dam, and the water flows out through slope failure of the southern slope together with the surface water of the second dam. The lilly trench will be further scoured by rainfall. There are silme deposits of several centimeter thick around the dam. It is obvious that the deposits flowed out due to rainfall on the slope.

(2) Pore Water Pressure Measurement

For estimation of saturation water level in the dam, water level was observed at each stage of boring works. Then, water head between the static water level and boring depth was obtained to estimate the pore water pressure. At the bottom of the hole strainer tubes were set for successive observation.

As the result of observation, water level in the hole BD-1, were GL-21.0m and GL-20.8m in the dry and rainy season respectively. In the hole BD-2 they were GL-14.4m and GL-14.2m respectively. There was little difference of water level between dry and rainy season. Consequently, it can be concluded that pore

water pressure did not increase in the rainy season compared to the dry season.

(3) Sampling and laboratory soil tests

Sampling of undisturbed samples of deposits with thin wall sampler around the dam and laboratory soil tests were carried out. The number of the samples for the laboratory soil tests and items of the tests are shown below. Sampling points are shown in Fig.3-6-2. The quantity is shown in Table 3-6-1.

① Laboratory soil tests

The results (Table 3-6-2) of the laboratory soil tests are summarized below.

- I) Water content measurement
- II) Specific gravity
- III) Grain size distribution
- IV) Density measurement
- V) Liquid limit test
- VI) Plastic limit test
- VII) Triaxis compression test
- VIII) Permeability test

③ The results of the soil tests

I) Measurement of specific gravity

The specific gravity of the soil particles of the dam embankment was 2.59 to 2.62, the average value of which was 2.61. The specific gravity of the deposits was 2.61 to 2.64, the average value of which was 2.63. These values are approximately the same as those of ordinary alluvial clay(2.6 to 2.8). Therefore, the samples are judged to be conglomerate of ordinary particles.

II) Water content and density measurement

Wet density(ρ_t) and natural water content(W) have close relation. They are shown together in the table 3-6-3.

Natural water content is higher in deposits than in tailing dam. Wet density is a little higher, too. ρ_t in ordinary alluvial deposits of sand is 1.60 ~ 1.80. Considering from this value, both materials are in dense condition.

iii) Grain size analysis

Curves of the soil of dam and the deposits are shown in Fig.3-6-3, showing that the distribution range of grains is between 0.005 mm and 0.425 mm, which means the grain size in this area is comparatively uniform.

The relation between uniform coefficient(U_c) and coefficient of curvature(U'_c) is as follows;

$U_c \geq 10, 1 < U'_c \leq \sqrt{U_c}$ (bad grading); 0 sample

$U_c < 10$, (uniform grading, bad grading) ; 4 samples

$U_c \geq 10, U'_c \leq 1$ or $U'_c > \sqrt{U_c}$; 0 sample

(composite grain size distribution, bad grading)

Judging from the analysis, whole samples are "poor grading".

iv) Liquid limit test and plastic limit test

The average values of the tests for the materials soil of dam and the deposits are shown in Table 3-6-4.

Compared with the values of the materials of the soil of dam and deposits, plasticity index of the material of the tailing dam is higher. This means that the deposits contains much silt, clay, and adhesive. However, consistency indices(I_c) which mean stability of soil are as follows;

soil of dam : $I_c=2.2 > 1$

deposits : $I_c=0.4 < 1$

These show the tailing dam is more stable than deposits.

v) Permeability test

The average permeability coefficients of the tailing dam and deposits are as follows;

Tailing dam $k=3.95 \times 10^{-3}$ cm/sec

Deposits $k=9.82 \times 10^{-5}$ cm/sec

The value of tailing dam is in the range of the ordinary permeability coefficient of sand to silt. On the other hand, the deposits are impermeable.

vi) Summary of the laboratory soil tests

The characteristics of the soil material of this tailing dam from the results

of the laboratory soil test are summarized as follows;

(tailing of dam)

- a) Distribution of particles is uniform and the grading is bad.
- b) The soil is comparatibly compact from density measurement
- c) Packing among soil particles is comparatibly stable.
- d) Permeability is the same as that of the ordinary silt to sand.

(deposits)

- e) Specific gravity and grain size are almost the same as those of the tailing dam. However, it contains much silt.
- f) Stability of soil is lower than that of the tailing dam.
- g) Permeability is lower than that of the tailing dam.

s

(4) Estimation of the section of the tailing dam

The geological cross section of the tailing dam was estimated from measurement of cross section and results of drilling test. The estimated cross section is shown in Fig.3-6-4. The boundary of dam and deposits could not be estimated from drilling test and soil test. Therefore, it was estimated by studying the bank construction of the dam as shown in Fig.3-6-5. Phreatic surface water was decided from drilling data and seepage position on the slope of the dam.

(5) The estimation of present stability of the tailing dam

① The stability of this tailing dam was estimated with the data abovementioned. The stability analysis and other studies are carried out according to "The construction standard of rubble/slime deposition mound and its explanation (Industrial Location and Environmental Protection Bureau, Ministry of International Trade and Industry, Japan).

1) Equation for stability calculation

Stability calculation of the tailing dam is carried out as follows;

$$F_s = \frac{\sum R(C' \cdot l + \{(W - U' \cdot b) \cos \alpha - K_h \cdot W \cdot \sin \alpha\} \tan \phi')}{\sum (R \cdot W \sin \alpha + K_h \cdot W \cdot h)}$$

F_s : safety factor

R : radius of sliding surface (m)

- W : weight per unit length of each slice (t/m)
- U' : static pore water pressure on the each sliding surface
(t/m²)
- U : pore water pressure on the sliding surface considered
to the excess pore water pressure by liquefaction (t/m²)
- Kh: design seismic coefficient
- b : width of slice(m)
- a : angle of vertical line and straight line connected from the
middle point of sliding surface to the center of circular arc of the
sliding surface (°)
- h : vertical distance between the center of gravity of each
slice and the center of sliding surface (m)
- l : length of sliding plane(m)
- ϕ, C' : adhesive power and internal friction angle, respectively,
calculated with effective stress(°, tf/m²)

ii) Phreatic surface

Phreatic surface of the tailing dam is assumed equal to the highest water level of the dam. Phreatic surface is estimated based on the hydraulic structures such as phreatic surface of deposits, foundation, drainage conduit and filter layer.

Phreatic surface during depositing and after completion of deposition is obtained by actual measurement.

② Stability analysis section

The section for stability analysis of the tailing dam is the section with highest phreatic surface according to "the Construction Standard of Tailing Dam". In case of this tailing dam, surface water does not usually exist, because of the termination of the dam. Therefore, the section of the western slope which has highest effective height and the steepest average gradient is selected for the stability analysis.

Stability analysis was carried out with a computer system. Stability analysis program is MINE/FS-1979. It is necessary to model the shape of the section. Model of the section shape is shown in Fig.3-6-6.

③ Soil constant

Soil constant of each zone for stability analysis of the tailing dam was decided by laboratory soil tests. However, as some dispersion was recognized in the test data, irregular data was eliminated from use.

i) sediments-1 (Zone-①)

These are coarse grained deposits classified with cyclone. Soil constant is as follows;

$$G_s = 2.61, \quad W = 14.8\%, \quad \rho_t = 1.736 \text{ g/cm}^3$$

$$\rho_d = \rho_t / \left(1 + \frac{W}{100}\right) = 1.736 / \left(1 + \frac{14.8}{100}\right) = 1.512 \text{ g/cm}^3$$

$$e = (G_s / \rho_d) - 1 = (2.61 / 1.512) - 1 = 0.727$$

$$G_s = 2.61, \quad W = 14.8\%, \quad \rho_t = 1.736 \text{ g/cm}^3$$

$$\rho_d = \rho_t / \left(1 + \frac{W}{100}\right) = 1.736 / \left(1 + \frac{14.8}{100}\right) = 1.512 \text{ g/cm}^3$$

$$e = (G_s / \rho_d) - 1 = (2.61 / 1.512) - 1 = 0.727$$

$$S_r = \frac{W \cdot G_s}{e} = \frac{14.8 \times 2.61}{0.727} = 53.1\%$$

From the values shown above, density in saturation ($S_r=100\%$) and water content are estimated as follows;

$$\rho_{sat} = (\text{weight of soil}) + (\text{weight of pore water})$$

$$= \rho_d + (1 - \rho_d / G_s)$$

$$= 1.512 + (1 - 1.512 / 2.61) = 1.933 \text{ g/cm}^3$$

Shear strength is as follows;

$$\phi = 30.0^\circ, \quad c = 0.00 \text{ tf/m}^2$$

ii) deposits-2 (Zone-②)

$$G_s = 2.63, \quad W = 35.7\%, \quad \rho_t = 1.774 \text{ g/cm}^3$$

$$\rho_d = \rho_t / \left(1 + \frac{W}{100}\right) = 1.774 / \left(1 + \frac{35.7}{100}\right) = 1.307 \text{ g/cm}^3$$

$$e = (G_s / \rho_d) - 1 = (2.63 / 1.307) - 1 = 1.012$$

$$S_r = \frac{W \cdot G_s}{e} = \frac{35.7 \times 2.63}{1.012} = 92.78\%$$

$$\rho_{sat} = \rho_d + (1 - \rho_d / G_s)$$

$$= 1.307 + (1 - 1.307 / 2.63)$$

$$= 1.810 \text{ g/cm}^3$$

Shear strength is as follows;

$$\phi = 23.0^\circ, \quad c=1.00 \text{ tf/ m}^2$$

④ Other conditions

i) seismic intensity

According to "Construction Standard of Tailing Dam", $K_h=0.15$ is adopted as horizontal motion during earthquake for strong motion area. Therefore, this value was used in this stability analysis.

ii) the center of circular arc

The center of circular arc was decided as follows.

Point A (X = 50.0, Y = 2388.0)

Point B (X = 110.0, Y = 2419.0)

Point C (X = 110.0, Y = 2479.0)

Point D (X = 50.0, Y = 2448.0)

Calculation of stability analysis was made with the centers of circular arc set up on the grids divided into $10\text{m} \times 10\text{m}$ area within the range above mentioned.

iii) Increments of circular arc

Increments of circular arc is $\Delta R=1.0 \text{ m}$.

⑤ Results of the calculation

Results of the calculation using the model (Fig.3-6-6) are shown in Table3-6-5. The detail of the results of stability analysis in ordinary condition ($K_h=0.00$), and the circular arc which gives minimum safety factor in each distance in the condition are shown in Fig.3-6-7 and Fig.3-6-8. And, the details of the results of calculation in case of earthquake ($K_h=0.15$) are shown in Fig.3-6-9 and Fig.3-6-10 respectively.

From the result, it is obvious that minimum safety factor of this tailing dam is less than 1.0 in both ordinary and earthquake conditions. In other sliding surfaces, almost all the safety factors in earthquake conditions are less than 1.0.

Therefore, stability of this tailing dam against slope failure is always considered to be in extremely bad conditions.

The reasons are as follows;

i) As regards prevention power of the dam, the section of the dam is too small to prevent.

ii) The gradient of the slope of the lower reaches is steep. From the reasons mentioned above, it is necessary to make immediate measure against the instability.

⑥ Judgement of danger by liquefaction

The dam has a risk of liquefaction in case of earthquake, because of the primary dam material is sand. It is necessary to judge the possibility liquefaction of the dam materials.

There are several standards judging the possibility of liquefaction. The simple methods are using N value, grain size distribution and uniform coefficient. General judgement is carried out by the simple methods at first. After that, in case of possible liquefaction, detailed methods must be carried out.

As regard to possibility of liquefaction, the methods mentioned below are described in "Construction Standard of Tailing Dam". According to the standard, in case of the following conditions, there are possibilities of liquefaction.

- i) The shallower part than 20 m below tailing dam surface.
- ii) The deeper part from phreatic surface.
- iii) The part of less than 20 of N value.

As to apply these conditions to this tailing dam, the part of ① in Fig.3-6-11 is to be applicable to i) and ii) above. However, N values are over 20. It does not satisfy the above conditions. Therefore, the liquefaction in this tailing dam is impossible.

3-7 Dust Problem

It is possible that the dust particles scattered by the wind from El Bote tailing dam have harmful effects on living conditions in and around the mining site. To analyze actual circumstances, various investigations were carried out with use of meteorological observation apparatus, dust collecting jars, low volume air samplers (LVS) and digital type dustmonotors.

3-7-1 Matters for Investigation

- (1) Meteorological survey with a self-recording anemometer
- (2) Measurement of dust density by LVS in the atmosphere
- (3) Dust sampling by dust jars and chemical analysis of the samples
- (4) Long term observation of dust density by digital type monitors at fixed points
- (5) Collection of existing meteorological records

3-7-2 Survey Results

The above-mentioned measurements were carried out separately in dry and rainy season in 1991 calendar year. These results are described below.

(1) Meteorological observation

Observation points are illustrated in Fig.3-7-1. The results obtained by the self-recording anemometer are summarized in Table 3-7-1. Table 3-7-2 and Table 3-7-3 show the daily records of wind velocity and direction during the survey period.

Self-recording anemometer was installed for continuous observation at the top of one shaft derrick of the mine, 300m east of the dam site. Results were recorded in a series of measurement periods, i.e., March 15-21, April 17-May 16, May 19-June 11 and July 19-25. The results during March 15-21, covering typical dry season, recorded 7.5m/s of the mean wind velocity, 16.0m/s as the maximum and 1.0m/s as the minimum. During this season the wind blows mainly from south and south-west (S ~ SW).

The results obtained from the rest of the periods, which mostly cover the rainy season of the year, recorded 1.2m/s of the mean velocity, 12.0m/s as the maximum and 0m/s as the minimum respectively. The wind also blows mainly from S ~ SW as in the dry period. Unlike the dry season, the wind often calms down to 0m/s from 8 a.m. in the morning till 20 p.m. in the evening.

(2) Dust jar

Dust jars were installed around the dam site as shown in Fig.3-7-2. Table 3-7-4 shows the measurement results.

BD-1 On the roof of the main office of El Bote mine, 50m east of the

tailing dam end

BD-2 Inside the farm land, 300m west of the dam

BD-3 On a hill side, south of the dam

BD-4 On the sand guard dam, 100m east of the dam

BD-5 On a sand guard dam, 200m north-west of the dam

BD-6 On a roof of a residence, west end of the city of Zacatecas.

The results of chemical analysis of these dust samples are summarized in Table 3-7-5.

These results indicate that heavy metal elements like Cu, Pb, Zn and Cd are concentrated at higher levels in the samples of BD-1, 4 and 5 than usually contained in the earth crust. In the samples of BD-2, 3 and 6, these heavy metals are not confirmed because the collected samples were too scarce to assay.

(3) Low volume air sampler(LVS)

Low volume air sampler was set as shown in Fig.3-7-3. Measurement conditions and the results are shown in Table 3-7-6 and 3-7-7 respectively.

Measurement was carried out for continuous 54.6 hours starting at 10:45a.m. on Jan. 18 till 17:00 p.m. on Jan.20. Total volume of the samples collected was 2.0mg, which is converted to 0.041 mg/m^3 of particle concentration in the atmosphere.

(4) Digital type dust monitor

Measurement was carried out at 36 fixed points for seven successive days starting March, 15. Measurement points and results are shown in Fig.3-7-4 and Table 3-7-8 respectively. The mean value, the maximum and the minimum are 25, 85 and 18 cpm respectively. Table 3-7-9 shows the relative concentration converted from the measurement data using F value obtained by LVS observation.

Fig.3-7-5 illustrates the areal distribution map of dust particles. A highly concentrated zone is observed in the north-eastern part from the tailing dam.

3-7-3 Dust Distribution in the Vicinity of El Bote Mine

From the El Bote tailing dam dust particles are blown up forming heavy sand storm when the wind velocity exceeds 10m/s. Especially, if the velocity is over 20m/s, it is impossible to walk on the lee side of the dam without dust

protection glasses. On the north-eastern slope of the dam, dust particles have been so accumulated that hinder the growth of plants and the living of animals.

Total volume of sand particles from the dam is greatly affected by the weather conditions. During the rainy season the dam surface is usually wet and this keeps the dust from springing up. Even if the surface is dried, particles are hardly carried away because of calm wind and heavy rain. Consequently, during the rainy season the dust problem may be left out of consideration.

In the dry season, on the other hand, the wind usually blows hard from S ~ SW with mean velocity of 10m/s and exceeds 20m/s instantaneously. The velocity normally reaches the highest at around 14p.m. in the afternoon. To understand the dust problem it is essential to analyse dust scattering pattern during the dry season.

For this purpose measurement results with digital type dust monitors at fixed points are summarized in Fig.3-7-5. As can be seen from this Figure, dust scattering pattern draws cocentrical arcs on the lee side, N ~ NE, from the dam. There exists a highly concentrated zone in this direction, 100m in width and 3km in length. It is clear that dust particles are carried away almost straight forward by the wind, not dispersed transversally. This suggests the possibility of dust falling in the city of Zacatecas if the wind blows hard with a velocity of 15m/s from NW direction.

As stated before distribution of the scattered dust is greatly affected by weather conditions. To know the past situation in this area meteorological data obtained through CNA (Comicion Nacional del Agua), a local authority of this field, were examined. Thus, such a wind condition as to carry the dust particles as far as the city of Zacatecas has never been found in the past six years (1985-1990). Consequently, it can be concluded that there is no direct influence of the dust from El Bote dam on the city of Zacatacas, nor on the farm land west of the dam.

Dust fall at the west end of Zacatecas (BD-6) can be estimated as 2.0 g/m^2 per month. Concentration of floating dust in the atmosphere is measured as 0.041 mg/m^3 with use of the LVS. The sample collected by LVS in the city is not sand particles but brown sooly substance. This may come from industrial or commercial activities inside the city.

Results of chemical analysis on the samples collected by the dust jars indicate that heavy metal elements like Cu, Pb, Zn and Cd are considerably concentrated in the dust compared to those contained in the average earth crust. When converted into a concentration ratio to aluminum content (Al=1.0), which is stable and regarded as one origin of the earth, these figures are as high as shown in Table 3-7-5. Thus, compared to the average earth crust, concentration ranges 35 ~ 75 for Cu, 250 ~ 920 for Pb, 130 ~ 360 for Zn and 500 ~ 940 for Cd respectively.

This high level of metal concentration may result from sulfide minerals, like galena and zincblend, remained in the flotation tailings. Consequently, if fine particles should reach the city or resident area, no matter how little volume may be, this could bring serious problems on environmental circumstance in this area.

As stated before, it is concluded that there is no direct or visible influence of dust particles on the city of Zacatecas at present. In the long term, however, possibility of air contamination, which could be brought by heavy metals transported with very fine particles, can not be denied completely. Therefore, some countermeasures are inevitable to prevent dust scattering from the dam.

3-8 Summary of Investigation

This area is formed on the Pimienta of Metasediments of Triassic Period. The River El Bote, main stream of the area, passes south of the El Bote mineral processing plant and tailing dam running toward northwest by west. As a result of the survey, ground water is likely to run underground along this river. In the rainy season ground water level rises by 0.6 ~ 0.8m with increased current movement.

Heavy metals are highly concentrated in surface water and soils almost all over the area because of natural mineralization. In soil samples, heavy metals like Cu, Pb, Zn, Fe, Cd, As and Hg are remarkably concentrated. In the samples of surface water Pb, Fe and Cd exceed the criterion limit of water supply standard set by EPA(USA) in many points. Especially, sample B-R2 show very lower pH value of 2 with extraordinarily high content of metal ions. Since this sample was taken from a branch river, upper stream from the tailing dam, it is

more likely affected by natural mineralization than the dam effluent. Furthermore, it may be suffered from other mining activity situated upstream from CFM.

Ground water is less contaminated than the surface, however, Pb and Fe exceed the criterion limit at several points. Cd is also near the limit.

Cyanide has not been detected from surface and ground water during the survey period.

A part of the tailing dam embankment has already collapsed due to landslide. Thus, an urgent counterplan is required on entire embankment. Study from the soil property tests also led to a conclusion that the dam stability was in so dangerous condition. Furthermore, in the rainy season, water could run on the dam surface flowing over the embankment. It is necessary to install suitable drainage system.

Influence of dust particles carried away by the wind from the tailing dam is another problem. In the dry season, violent sand storm blows almost continuously toward the northeastern valley due to heavy wind from south or south-west. This greatly affects living conditions in the vicinity. Because of nearly constant wind direction, neither the city of zacatecas nor the farmland west of the dam suffer from this dust problem at present. However, as the dust particles contain some metal elements like Pb and Zn, it is required to carry out longer term measurement and study the influence on human body. Without reference to further study some countermeasures against dust scattering should be done urgently.

3-9 Measures against Mine Pollution

3-9-1 The counterplan against slope failure of the tailing dam.

(1) Selection of counterworks

The reasons of instability of this tailing dam are as follows;

- ① Steep gradient of slope
- ② Weak prevention power of initial embankment

The counterworks must be examined based on the above reasons.

To remove the origin of instability, the following works are considered.

- ① Earth removal work ; remove soil to reduce overload of soil mass.
- ② Counter weight fill work ; make fill-bank on the toe of the slope to prevent

land slide motion by resisting power of fill-bank soil.

- ③ Use earth removal work together with counter weight fill work
- ④ Prevention work ; to increase shear resistance by pile work or anchor work

(2) Optimum counterplan

These works shown above are generally considered. In case of this tailing dam, counter weight fill work is recommended from the following reasons.

- ① Part of initial embankment is comparatibly packed. However, as consolidation settlement has not been progressed on the slime sediments, soft sediments still remain. Therefore, earth removal work is difficult to perform.
- ② The surface of dam slope is compatibility hard by some working. The firm surface prevents scattering of powder dust, penetration of water and scouring of slope, etc. Therefore, it is better for the work to leave the shape of the tailing dam as much as possible.
- ③ To cover with soil the whole tailing dam by counter weight fill work increses the stability of the dam, and the work is effective as the measure against mine pollution such as powder dust and water pollution.
- ④ As there are banking materials near the dam, counter weight fill work is also economical.

(3) Model Cross Section of Counter Weight Fill Work

Model cross section of Counter weight fill work is shown in Fig.3-9-1. Considering stability of slope, inclination of slope is 40% and the steps with 5 m width is installed every 10 m height.

Sewage flown out from the toe of slope of the dam is led to outside of the dam with closed drain ditch. Rocks near planned new tailing dam site will be crushed to be banking material. This work also helps to make the new dam hold bigger pondage.

But, the total area of the fill bank in this section is about 950m^2 , only in the western slope, length of the dam is about 350m, the amount of fill bank is about $330,000\text{ m}^3$. This is a very big amount. Therefore, fill bank is necessary to be performed deliberately from lower to upper.

(4) Stability Test

The target stability after completion of the counter weight fill work was over 1.2($F_s \geq 1.2$). The equation and program for the stability analysis was applied under the same conditions used as in "present stability analysis".

Cross section for stability analysis is shown in Fig.3-9-1

① Soil constant and other conditions

Soil constant of each zone shown in Fig.3-9-2 is the same as that already used in the article "3-6 Tailing Dam". Constants of gravelly soil for the counter weight fill work are decided as follows based on "Construction Standard of Tailing Dam" and other documents because of no actual data.

$$\rho_d = 1.800 \text{ g/cm}^3$$

$$\rho_{sat} = 1.912 \text{ g/cm}^3$$

$$c = 0.00 \text{ tf/m}^2$$

$$\phi = 37.0^\circ$$

Horizontal seismic intensity during earthquake($K_h=0.15$) and increments of circular arc($\Delta R=1.0 \text{ m}$) are the same values as in article "3-6. Tailing Dam".

The center of circular arc are set up within the following range.

Point A (x= 10.0 Y=2395.0)

Point B (x=100.0 Y=2435.0)

Point C (x=100.0 Y=2525.0)

Point D (x= 10.0 Y=2485.0)

② Result of calculation

The calculation result with the analysis model shown in Fig.3-9-2 is shown in Table 3-9-1. The detail in ordinary condition and circular arcs which give minimum safety factor in each distance are shown in Fig.3-9-3 and Fig.3-9-4, respectively. The detail of calculation results during earthquake($K_h=0.15$) are shown in Fig.3-9-5 and Fig.6-9-6.

The detail of calculation results during earthquake($K_h=0.15$) are shown in Fig.3-9-5 and Fig.3-9-6.

Minimum safety factor satisfies the target value, i.e. over 1.2. Therefore, the stability shown in the Model Cross Section in Fig.3-9-1 can be decided to have "No problem".

3-9-2 Measures for drainage

As the result of survey, it became obvious that rainwater flowing on the surface of the dam in rainy weather causes the scouring of the dam surface and outflow of soil through the scoured part of the dam.

The proper measures against this phenomena is to install the drainage facilities in order to collect and discharge the surface water. However, it is necessary to take permanent measures against surface water pollution, because use of this dam has already been finished. That is, the rain water in the dam must be prevented from contact the polluted soil of the dam, For this purpose, it is necessary to cover the dam surface without polluted soil and to install drainage channels after the covering.

The specification of the work for prevention of the pollution is described below.

(1) Soil spreading work

The gravelly clayey soil is used in this work. The soil distributes in the south-western part of the dam and in the opposite side of the temporary using dam. Spreading depth is about 30 ~ 50 cm and inclination of the spreading is about 2 % toward drainage.

(2) Drainage

The outside Drainage canal, inside drainage canal and emergency drainage canal are usually installed. However, the outside drainage is not installed, because the area of water collecting on the dam surface is almost negligible. Whole area of water collecting is also narrow as 0.03 km², the emergency drainage is not installed. Only ordinary drainage is installed.

U type Colgate flume which is comparatibly strong against settlement and horizontal moving is used, because the inside drainage is installed on the depositing surface. Polyethylene pipe is used outside of the dam.

The design of drainage inside of the dam is shown in Fig.3-9-7.

(3) Drainage capacity

Drainage capacity for surface water inside of the dam is decided by the amount of precipitation flowing into the dam estimated by probable recipitation

amount for 100 years (The expected maximum amount of precipitation once every 100 year).

① Probable precipitation amount in a day

The arranged maximum precipitation data per a day in La Bufa observatory during 1981 ~ 1991 is shown in Table.3-9-2

The data plotted on the logarithmic probability graph is shown in Fig.3-9-8. Probable precipitation amount for 100 years(R24) is obtained by Fig.3-9-8;

$$R_{24}=100 \text{ mm/day}$$

② Water collecting area

Water collecting area of each drainage is as following;

$$A_1=0.03 \text{ km}^2 \quad (\text{ first tailing dam })$$

$$A_2=0.002 \text{ km}^2 \quad (\text{ second tailing dam })$$

③ Run-off time

The equation is shown below;

$$\begin{aligned} T_1 &= 1.67 \times 10^{-3} (L/\sqrt{S})^{0.7} \\ &= 1.67 \times 10^{-3} (200/\sqrt{1/50})^{0.7} \\ &= 0.27(\text{h}) \end{aligned}$$

$$\begin{aligned} T_2 &= 1.67 \times 10^{-3} (50/\sqrt{1/50})^{0.7} \\ &= 0.10(\text{h}) \end{aligned}$$

T; reaching time (hour)

L; distance of flowing from farthest point (m)

④ Average maximum precipitation intensity

The equation is shown below;

$$\begin{aligned} R_1 &= \frac{R_{24}}{24} \times \left(\frac{24}{T} \right)^{2/3} \\ &= \frac{100}{24} \times \left(\frac{24}{0.27} \right)^{2/3} \\ &= 83 \text{ mm/h} \end{aligned}$$

$$\begin{aligned} R_2 &= \frac{R_{24}}{24} \times \left(\frac{24}{T} \right)^{2/3} \\ &= \frac{100}{24} \times \left(\frac{24}{0.10} \right)^{2/3} \\ &= 161 \text{ mm/h} \end{aligned}$$

R ; Mean maximum precipitation intensity (mm/h)

R24; (designed)precipitation amount per a day (mm)

⑤ Design amount of flood

The equation is shown below;

$$Q_p = \frac{1}{3.6} \times f \times R \times A$$

Qp ; maximum amount of flood (m³/sec)

f ; coefficient of flow (grassland and forest 0.8)

A ; area of basin

The maximum amount of 1st tailing dam and 2nd tailing dam are as follows;

$$Q_{p1} = \frac{1}{3.6} \times 0.8 \times 83 \times 0.03$$
$$= 0.55 \text{ m}^3/\text{sec}$$

$$Q_{p2} = \frac{1}{3.6} \times 0.8 \times 161 \times 0.02$$
$$= 0.72 \text{ m}^3/\text{sec}$$

(4) Section of drainage

Drainage inside of the tailing dam is U type Colgate flume. For decision of the size of the Colgate flume, next equation is used.

$$v = \frac{1}{n} \cdot R^{2/3} \cdot I^{1/2}$$

$$Q = vA = \frac{1}{n} \cdot A \cdot R^{2/3} \cdot I^{1/2}$$

Q ; outflow(m³/sec)

v ; current velocity (m/sec)

A ; area of section of the rate of flow (m²)

R ; A/L(m)

L ; (m)

I ; hydraulic gradient (%)

n; coefficient of coarseness (n=0.022)

By assumed section of drainage shown in Fig.3-9-9;(500 x 250)

$$A=0.469 \text{ m}^2$$

$$R^{2/3}=0.400$$

$$I=0.02$$

$$n=0.022$$

To substitute these value for Manning's equation;

$$Q = \frac{1}{0.022} \times 0.469 \times 0.400 \times 0.02^{1/2}$$
$$= 1.206 \text{ m}^3/\text{sec}$$

Compared to the design flood amount of 1st dam and 2nd dam;

- $Q=1.206 \text{ m}^3/\text{Sec} > Q_{p1} = 0.55 \text{ m}^3/\text{Sec} \dots\dots\dots 0.K$
- $Q=1.2066 \text{ m}^3/\text{Sec} > Q_{p2} = 0.72 \text{ m}^3/\text{Sec} \dots\dots\dots 0.K$

Therefore, to use the Colgate flume with section shown in Fig.3-9-9 is decided. The water through the Colgate pipe is led to the outlet through polyethylene pipe with ϕ 400 mm.

3-9-3. Measure against Dust Scattering

Powder dust due to drying of the dam surface scatters in the dry season. The following three works for prevention from the powder dust scattering are considered.

- (1) Sprinkling work: to sprinkle water with sprinkler.
- (2) Surface hardening work: to harden the surface by sprinkling of chemical liquid.
- (3) Planting treatment: to plant vegetation with spraying of seeds or turfing lawns
- (4) Soil covering work: to cover with soil on the dam surface.

The permanent measures against pollution are necessary, because the use of this tailing dam has already been finished. And, taking measures against the dam collapse and drainage problem are also necessary together with the measures against powder dust scattering at the same time. As the results of examination with consideration to the issues mentioned above, soil covering work is considered to be the most suitable measure against powder dust scattering.

As regards soil covering work, counter weight fill work on the surface of the dam slope and soil covering work on the upper surface of the dam are

performed, according to the chapters "3-9-1 Measures against the Dam Collapse" and "3-9-2 Measures against Drainage of the Dam".

3-9-4 Measures against Groundwater Pollution

By the hydraulic observation, El Bote river water percolates underground in the downstream area from El Bote tailing dam. Chemical contents of river water and groundwater is higher than the usual background due to influence of veins and mineralization zone. But, Infiltration of waste water from tailing dam and mineral dressing plant does not affect to the groundwater pollution.

However, it is considered that the polluted groundwater flows down to the pumping up well of the Zacatecas city easily, with the condition of ① small amounts of rainfall in long terms and

② increasing of population and industries in the Zacatecas city after the consideration of

① formerly said groundwater flow characteristics, that is, event water runs on the surface of aquifer easily, and

② the present distribution of groundwater potential is formed by small taking of groundwater from the pumping up well. We have make a observation of groundwater behavior between the El Bote mine and this well, and monitor the quality of the pumping up groundwater.

The waste water of the mine does not control the groundwater property at the present time, but the following measures should be done to prevent the pollution in the future.

The first measure is to cover tailing dam by soil covering and planting to decrease dissolution of dam material by infiltration of rainwater. The second is to flatten the deposit plane for rapid evaporation of waste water. The third is waste water recycle to prevent the infiltration of pollutant to the downstream.

3-9-5 Work Program and Construction Cost

Work program and construction cost for completion of each countermeasure plan are roughly estimated as follows.

(1) Work program

Work program is illustrated in the figure shown below.

Type of Work	Amount	5month	10month	15month	20month
Counter Weight Fill Work	580,000 m ³		22 month		
Soil Covering Work	20,000 m ³	2.2month			
Drainage Inside The Dam	290 m	0.8month			
Drainade Outside The Dam	450 m	0.2month			

(2) Construction Cost

According to the construction basis in Mexico, total costs are estimated as follows.

Type of Work	Amount	Unit Cost (US\$)	Total Cost (US\$)
Countermeasures against Dam Collape and Dust Problem			
Counter Weight Fill Work	580,000 m ³	6.3	3,654,000
Soil Covering Work	20,000 m ³	4.0	80,000
(Sub Total)			(3,734,000)
Drainage			
Inside the Dam	290 m	120.0	35,000
Outside the Dam	450 m	113.3	51,000
(Sub Total)			(86,000)
TOTAL			3,820,000

(3) Specification of Work

Specification of the works and necessary equipment are listed in the following Table.

Type of Work	Equipment	Unit Capacity	Unit
Counter Weight Fill Work			
Rock excavation at borrow pit	Bulldozer with Ripper (32t class)	53 m ³ /h	3
Loading of crushed rock	Backhoe (1.0m ³ class)	51 m ³ /h	3
Transportation	Dumptruck (11t class)	17 m ³ /h	9
Spread and Roll	Bulldozer (21t class)	64 m ³ /h	3
Cutting at the borrow pit	by manpower		
Soil Covering Work			
Excavation and loading of clayey soil	Backhoe (0.6m ³ class)	41 m ³ /h	1
Transportation	Dumptruck (11t class)	18 m ³ /h	3
Spread and Roll	Bulldozer (11t class)	41 m ³ /h	1

Remarks

1. Transportation during the Counter Weight Fill Work is estimated as 1km.
2. Transportation during the Soil Covering Work is estimated as 0.7km.
3. Working hours are 7 hours a day and working days are 25 days per month.

